Report C87A-25

ADVANCED DOUBLE LAYER CAPACITOR

Prepared by:

Anthony B. LaConti, Ph.D.
Philip Lessner, Ph.D.
S. Sarangapani, Ph.D.

GINER, INC.
14 Spring Street
Waltham, MA 02254-9147
(617)899-7270

October, 1989

5th Quarter Interim Technical Report

May 1, 1989 to July 31, 1989

Contract No. N00014-88-C-0391
ARPA Order No. 9526

Prepared For:

OFFICE OF NAVAL RESEARCH
Department of the Navy
800 N. Quincy Street
Arlington, Virginia 22217

The views and conclusions contained in this document are those of the authors and should not be interpreted as necessarily representing the official policies, either expressed or implied, of the Defense Advanced Research Projects Agency or the U.S. Government.

THIS DOCUMENT HAS BEEN APPROVED FOR PUBLIC RELEASE AND SALE. ITS DISTRIBUTION IS UNLIMITED WITH THE EXCEPTION OF THE APPENDIX WHICH IS LIMITED TO GOVERNMENT PERSONNEL.

TABLE OF CONTENTS

LIST OF TABLES AND FIGURES

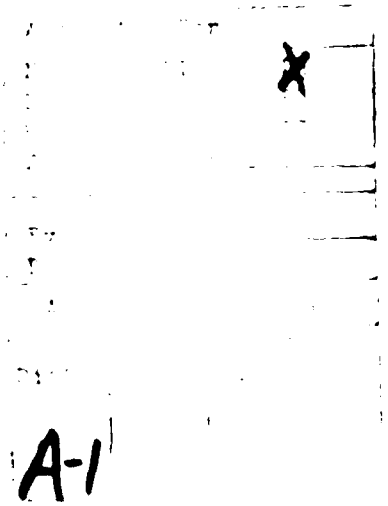

A-1

GINER, INC. 14 SPRING STREET • WALTHAM, MASSACHUSETTS 02254-9147 • (617) 899-7270

1. TECHNICAL OBJECTIVES

The overall goal of this project is to develop electrochemical capacitors with no liquid electrolyte present. The liquid electrolyte is replaced by a solid ionomer electrolyte. An advantage of these devices over conventional electrochemical capacitors containing free acid would be greater safety and reliability.

In the fifth quarter, we concentrated our efforts in five areas: 1) preparation and characterization of electrode materials, 2) fabrication of membrane and electrode (M and E) assemblies, 3) development of sealed-cell hardware, 4) capacitance determination by constant load discharge, and 5) determination of cell internal resistance.

2. EXPERIMENTAL METHODS

2.1 Preparation and Characterization of Electrode Materials

2.1.1 Preparation

The thermal method was used to prepare RuO_x. Baseline conditions call for heating the $RuCl_3$-$NaNO_3$ mixture to 500°C for 3 hours, followed by slowly cooling the mixture to room temperature. The effect on the surface area of the resulting RuO_x powder when quickly quenching the mixture in water was studied.

Ruthenium and iridium oxides show mutual solubility over the entire range of composition (Balko, et al., 1980). A mixed (50 at%) Ir,Ru oxide was prepared from a mixture of $IrCl_3$ and $RuCl_3$ in $NaNO_3$ at 500°C for 3 hours. The mixture was quenched in water after removal from the oven.

RuO_x was also prepared from a $CsNO_3$ flux. Other preparation parameters were the same as for the $NaNO_3$ flux method.

2.1.2 Surface Area

Surface area measurements on RuO_x samples were done using a Micromeretics FlowSorb II 2300 apparatus, as described in the 3rd Quarterly Technical Report.

GINER, INC. 14 SPRING STREET • WALTHAM, MASSACHUSETTS 02254-9147 • (617) 899-7270

2.1.3 Transmission Electron Microscopy

Transmission electron microscopy (TEM) was done to determine the fine structure of the RuO_x powders. The RuO_x samples were dispersed on Holey Film supports. All TEM work was done at Eastern Analytical Laboratories (Billerica, MA).

2.1.4 Scanning Electron Microscopy

Particle size analysis was done by computer-assisted SEM. The image analyzer determines the size of particles within a given field.

2.1.5 X-Ray Diffraction

RuO_x and $(Ru,Ir)O_x$ samples were sent to Oneida Research Services (Whitesboro, NY) for X-ray powder diffraction. A copper X-ray source was used. Samples were scanned over a 2-θ range of 4 to 94° with a 0.05° step angle.

2.2 Preparation of M and Es

Electrodes continued to be prepared by using a modified proprietary Giner, Inc. method.

RuO_x-Nafion slurries were also made with the addition of a small amount of wetting agent (Triton X-100).

2.3 Cell Hardware

During the 3rd and 4th Quarters, hardware was developed that allowed M and E testing with no liquid electrolyte present. A water reservoir around the outer edge of the M and E kept the M and E hydrated.

This quarter, we have developed sealed-cell hardware that requires no water reservoir. An exploded view of the cell is shown in **Figure 1**. The M and E assembly (8) consists of RuO_x-Nafion electrodes on each side with an annular Pt-air reference electrode on one side. Contact to the two electrodes and the reference electrode is made via gold-plated titanium sheets (4, 6 and 10). Gold wires are welded to the sheets and brought out through feedthroughs to make contact to the external circuit. Teflon gaskets (3, 5, 7, 9, and 11) prevent the contact plates

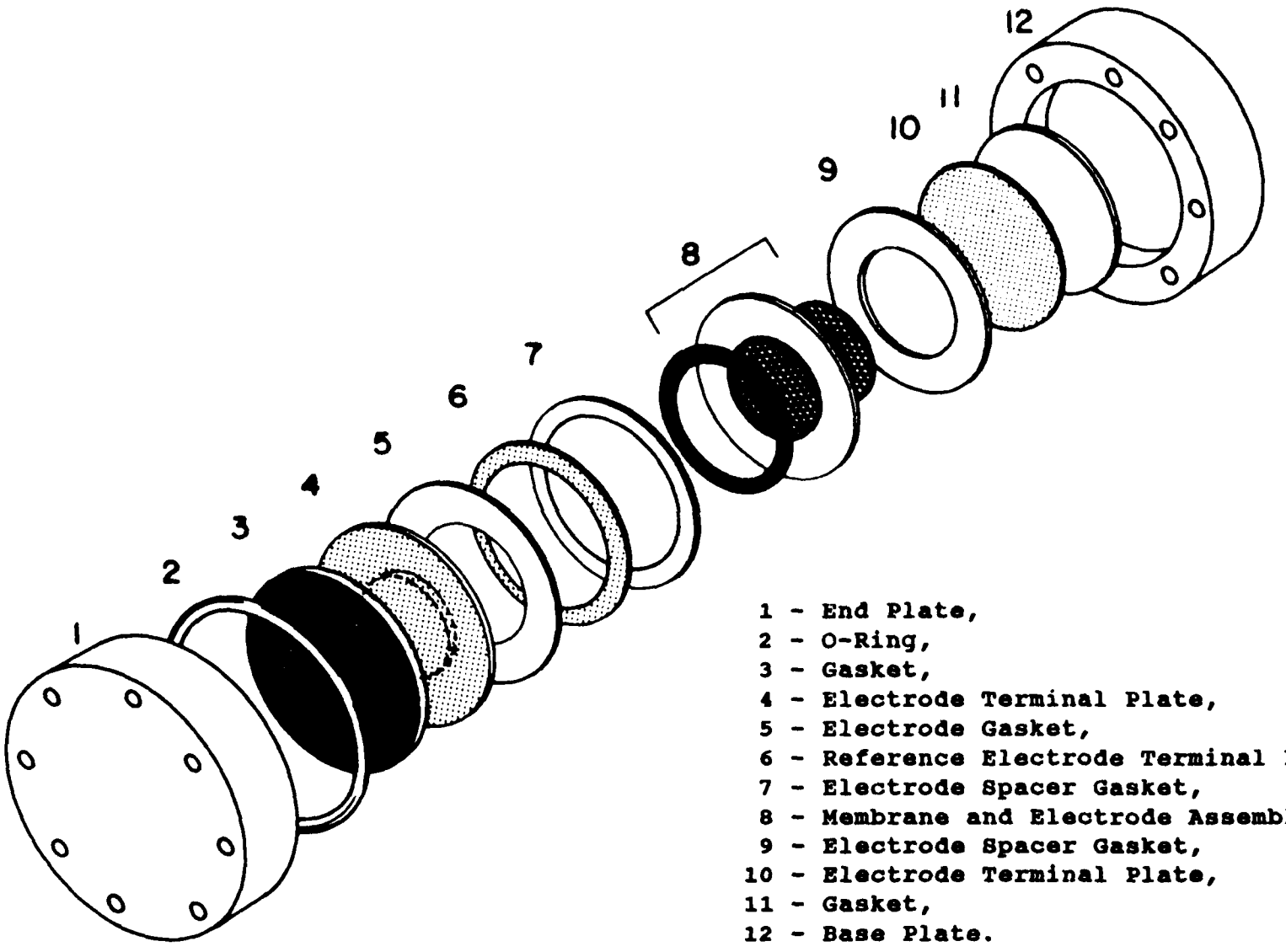

1 - End Plate,
2 - O-Ring,
3 - Gasket,
4 - Electrode Terminal Plate,
5 - Electrode Gasket,
6 - Reference Electrode Terminal Plate,
7 - Electrode Spacer Gasket,
8 - Membrane and Electrode Assembly,
9 - Electrode Spacer Gasket,
10 - Electrode Terminal Plate,
11 - Gasket,
12 - Base Plate.

Figure 1: Sealed-Cell Hardware

from touching each other and the exposed membrane. The entire package is sealed with an O-ring (2). The initial design used polysulfone end plates (1 and 12), but we later switched to polypropylene due to suspected high water transport through the polysulfone.

2.4 Cell Testing

Characterization of the electrodes during the first year of the contract was done primarily by cyclic voltammetry. This allowed us to determine individual electrode capacitances by methods explained in detail in the first four quarterly reports. Although this method has been continued to be used during this quarter, we have begun to transition into testing complete M and E assemblies by discharge through a constant resistance load. A block diagram of the experimental arrangement is shown in **Figure 2**. The cell is charged via a potentiostat (+0.9-1 V). The cell is then switched to discharge through a precision resistor. The voltage across the resistor is recorded as a function of time on an y-t recorder. Capacitance and charge storage are determined from the V vs. t (or i vs. t) transients.

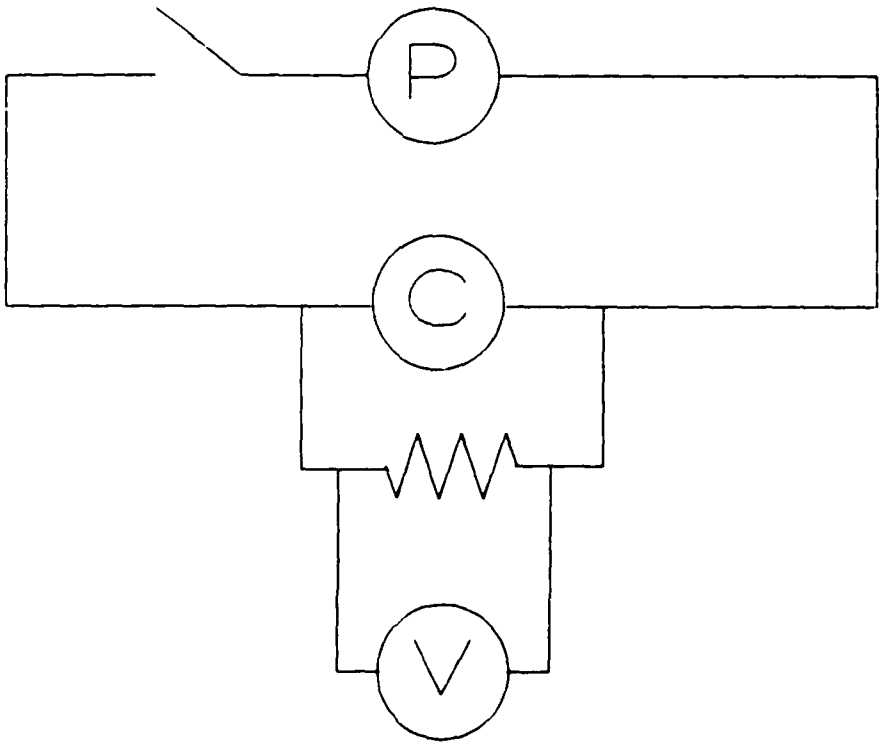

Figure 2: Block Diagram of Cell Charging and Discharging Circuit, P - Potentiostat, C - Cell, V - Voltmeter or y-t recorder.

GINER, INC. 14 SPRING STREET • WALTHAM, MASSACHUSETTS 02254-9147 • (617) 899-7270

Internal resistance (or equivalent series resistance ESR) is determined using a current interruption. A square wave cathodic pulse is applied to the cell electrodes. The voltage at the instant the current switches is measured and Ohm's law is used to compute resistance.

3. RESULTS AND DISCUSSION

3.1 Electrode Materials

Table I lists the electrode powders prepared this quarter. In all cases, the starting salts were mixed with the flux material in the form of a slurry. Transformation was carried out at 500°C for 3 hours. Standard procedure established in the program had been to turn off the oven and let the molten mixture slowly cool. Powder 369-14A was removed from the oven after 3 hours and cooled rapidly in air (10 to 15 minutes). The surface area of 96 m²/g was only slightly higher than the 85 m²/g produced in the best slow-cooled case. Powder 369-14B was therefore cooled by plunging the molten mixture into water. The 115 m²/g was significantly better than that obtained in the air-cooled cases. The water quenching procedure was adopted as standard for the further preparations.

Table I - Electrode Powder Preparation

Powder No.	Salt(s)	Flux	Cooling Method	Surface Area (m²/g)
369-14A	$RuCl_3$	$NaNO_3$	Air	96
369-14B	$RuCl_3$	$NaNO_3$	Water	115
369-31	$IrCl_3$ $RuCl_3$	$NaNO_3$	Water	149
369-47	$RuCl_3$	$CsNO_3$	Water	66

Examination of Powder 369-14A and 363-74 (95 m²/g - see 4th Quarterly Report, Table I, for preparation conditions), showed they had similar morphology to that observed in earlier powders. Porous RuO_x particle aggregates are made up of crystallites that are on the order of 100 Å.

[illegible]

[illegible]

[illegible]

[illegible]

[illegible]

[illegible]

[illegible]

[illegible]

[illegible]

[illegible]

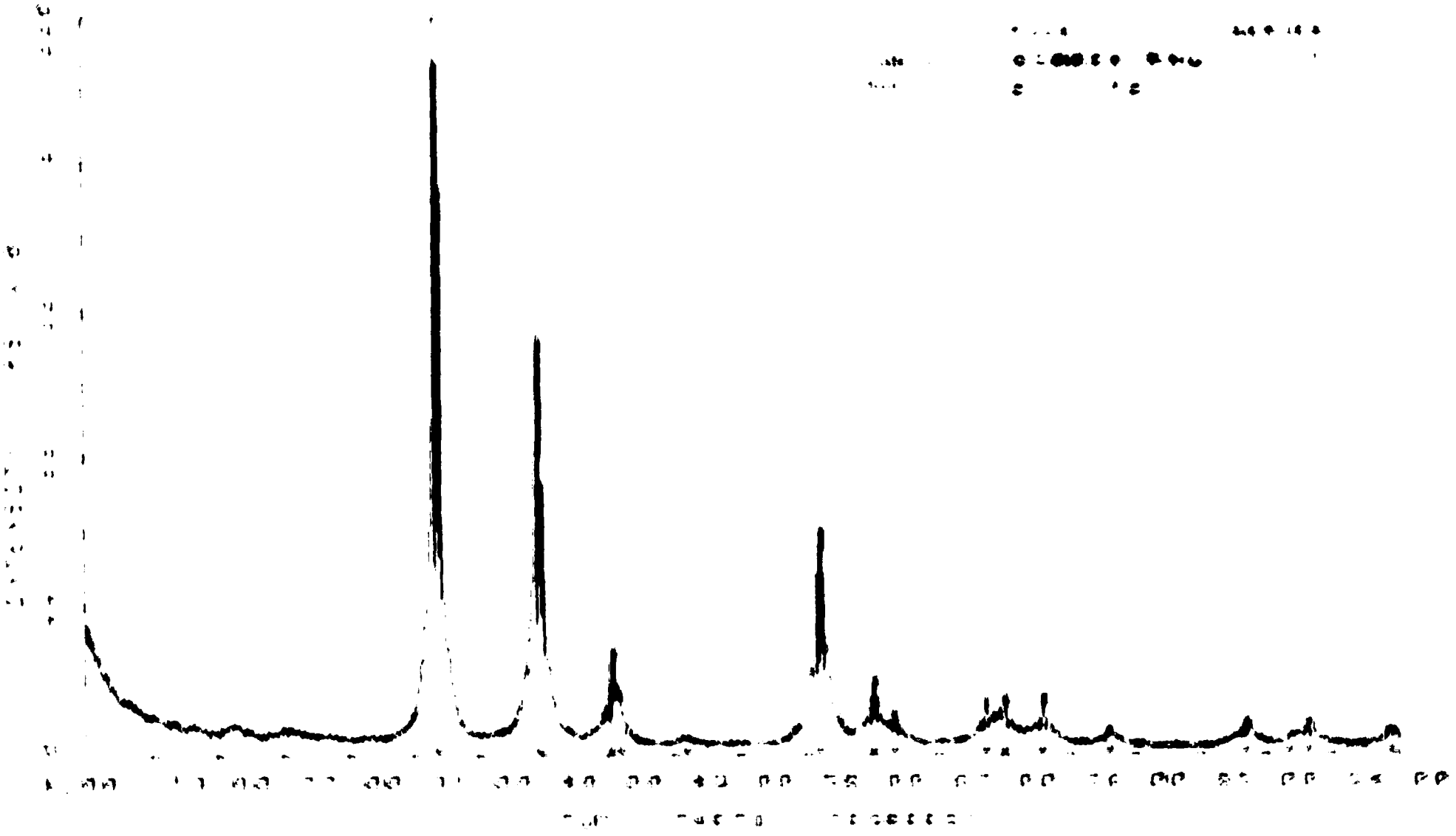

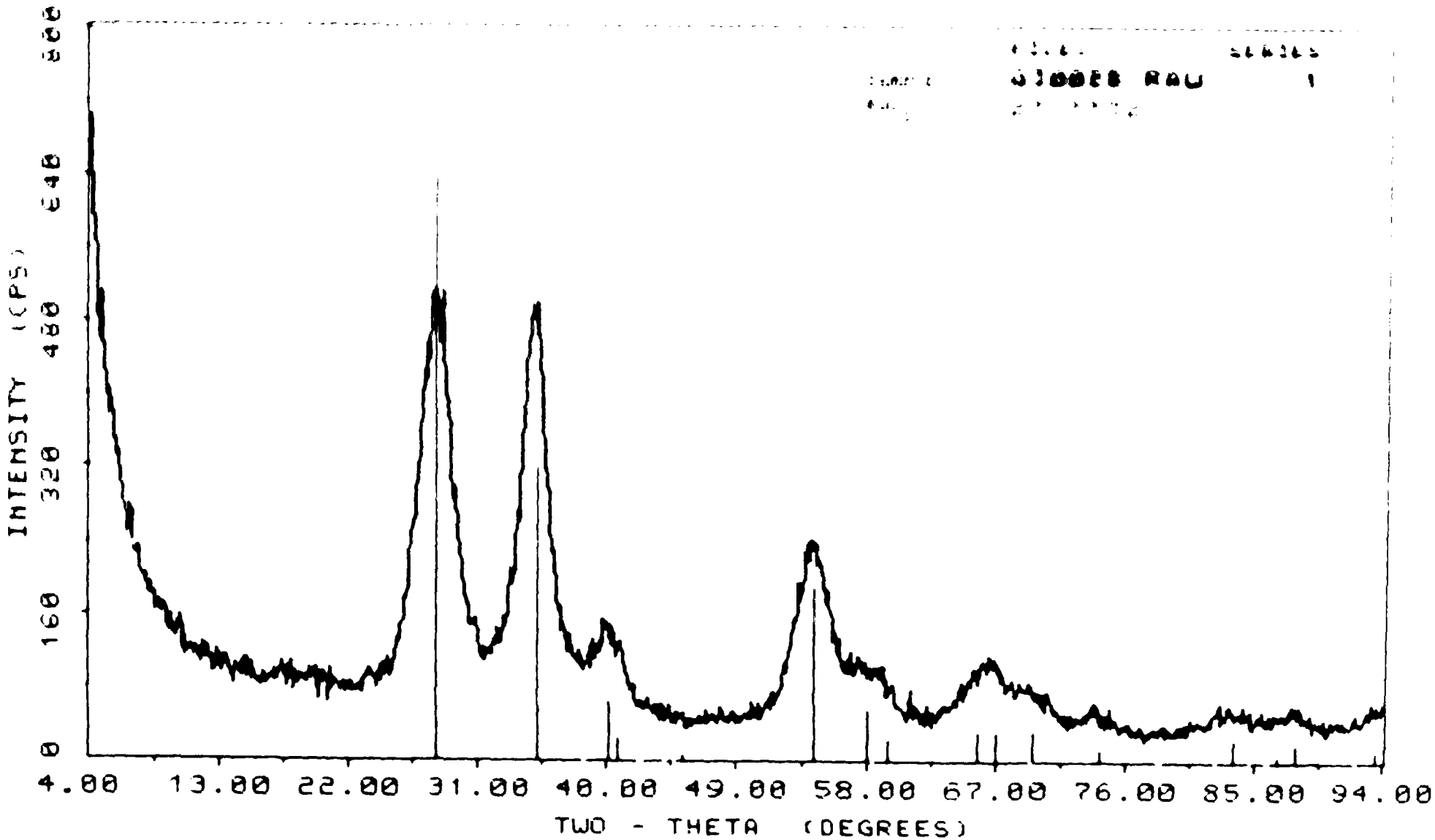

Figure 5: X-Ray Diffraction Pattern for Powder 369-31 ($(Ru,Ir)O_x$).

To prove this hypothesis, we carried out an experiment with a Solartron Frequency Response Analyzer (FRA). **Figure 6** shows the impedance spectrum obtained with a Solartron FRA coupled with a Solartron potentiostat. The electrode was an M and E (which has an even lower impedance than the RuO_x-sprayed disk we experimented with before), with a Pt/air reference electrode bonded to it. The impedance spectrum is very characteristic of this type of system with a clear semicircle and diffusional part.

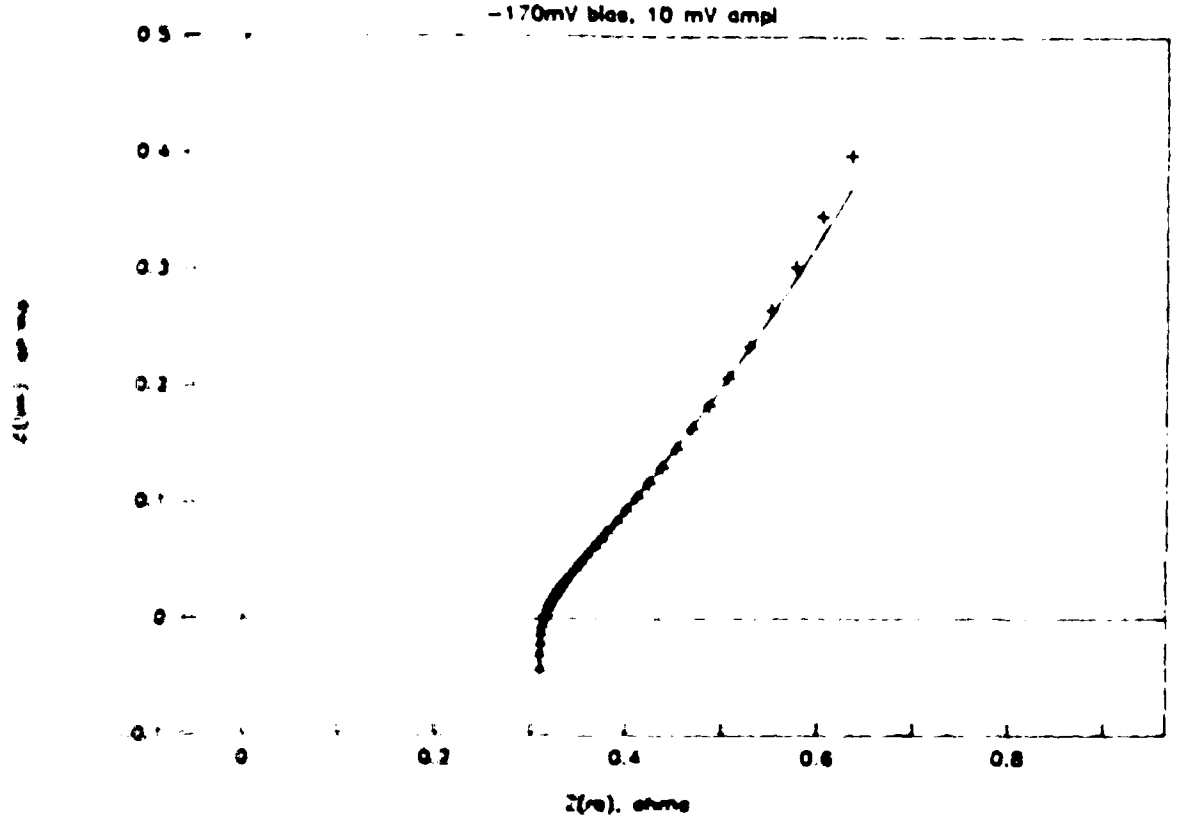

Figure 6: Impedance Data and Calculated Fit Obtained with Solartron 1250 FRA with 1286 Electrochemical Interphase, on Electrode 356-72-1, at 1.0 cm², 10 mg/cm² Loading of RuO_x. 5 wt% Nafion was used to make the electrode. The reference electrode was a Pt/air electrode, placed onto the Nafion 117 Membrane. +, Experimental Data; —, Fit to Data.

The impedance of an ideal capacitor is given by -j/wC. When the impedance of a capacitor is plotted in the complex plane, one obtains a straight line with the imaginary value of the impedance increasing with decreasing frequency. If a series resistance is added to this capacitor, then the straight line is displaced by

the value of the resistance in the real axis. A resistance parallel to the capacitor gives a semicircle. The high frequency intercept of the semicircle on the real axis gives the series resistance. Electrochemical systems also possess impedance attributable to the diffusional process. The diffusional impedance cannot be represented by a simple equivalent circuit. This impedance, also called the Warburg impedance, results in a 45-degree angle when the imaginary values of the impedance are plotted against the real values. In other words, over the frequency range in which the diffusional process becomes rate limiting, the values of real and imaginary parts of the impedance are equal.

Earlier work on the impedance of RuO_x electrodes has shown that the impedance of this system can be represented by the following equivalent circuit:

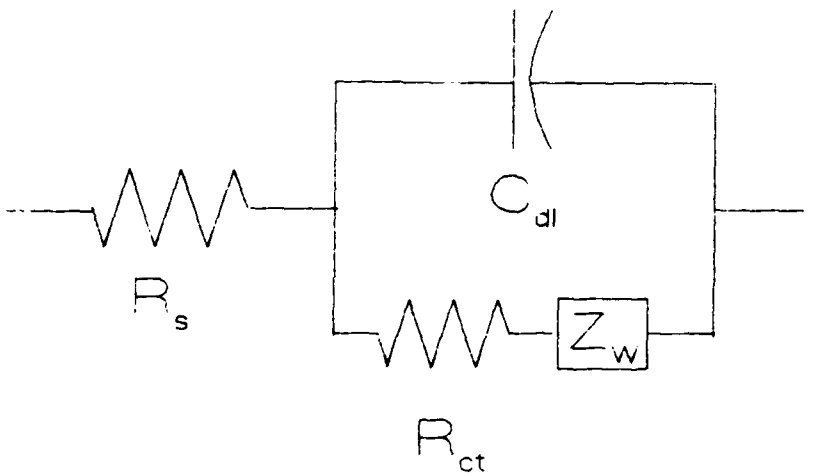

In principle, the charge storage can arise from a) the double-layer charging, b) the charge transfer process involving protons and the surface oxide layer, and c) the bulk reaction involving protons and bulk RuO_x. In practice however, one or the other process alone may be observable, depending on the frequency interval and on the electrode bias potential. Let us analyze the data obtained from the Solartron FRA.

The equivalent circuit for the data represented in Figure 6a should include a series inductance, and the resulting circuit is:

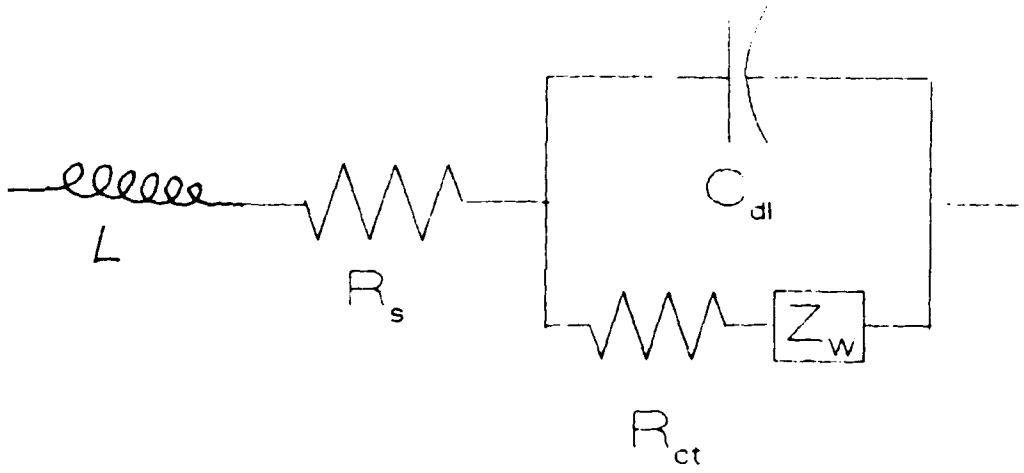

Analysis of the data using Abbey's impedance analysis program (Kyburz Abbey, 1989) gives the following values for the components of the equivalent circuit:

$L = 1.5 \times 10^{-7}$ H
$R_s = 0.303$ ohm
$C_{dl} = 4.28 \times 10^{-4}$ F
$R_{ct} = 1.6 \times 10^{-2}$ ohm
$Z_w = 5.83$ ohms

Figure 6 shows the fit of impedance values calculated using the above equivalent circuit to the actual data. The fit is excellent except at frequencies less than 30 Hz. The capacitance value of 0.4 mF/cm² is rather low compared to a value of 33 mF/cm² obtained from cyclic voltammetric data. This low number is a value obtained from the semicircle observed in the frequency range 1-13 kHz, and reflects the double layer and other capacitive component of the fast-charge transfer process (Rïshpon and Gotterfeld, 1984). The Warburg or the constant-phase element shows a relatively high value of 6 ohms, indicating the large capacitive contribution arising from the low frequency processes such as the slow-charge transfer reaction, i.e., the movement of charge into the sublayers of the spherical particles. These measurements provide a way to assess the available charge for a fast-dischrage (submillisecond duration) application. The above interpretation of the impedance data agrees well with that reported in the literature and also with our own pulse discharge data. The pulse data do show clearly at least two time constant processes, one in the millisecond time range, and the other at seconds range. In the coming quarters, further attention will be paid to acquiring and understanding data at higher frequencies.

The foregoing discussion shows that in order to get acceptable data for impedance analysis of the RuO_x capacitor systems, we need instrumentation that will support such low impedance measurements. Since the Solartron instrument was a demo model obtained for this purpose, further work was not possible in this direction.

3.2.3 Full Cell Testing

Two M and E assemblies were made and assembled into the sealed-cell hardware shown in Figure 1. Cells were tested by charging and discharging in the configuration shown in Figure 2. **Table II** lists the fabrication parameters for the M and Es and the cell hardware used.

Table II - Cell Builds

M and E	Cell Hardware
369-20-1	Polysulfone
369-38-1	Polypropylene

A typical discharge curve for M and E 369-38-1 is shown in **Figure 7a**. **Figure 7b** plots the same curve on a semilogarithmic scale. If the circuit could be represented by the equivalent circuit shown in **Figure 8**, then the voltage across the external resistor as a function of time would be:

$$V_L = ae^{-bt} \qquad [1a]$$

with

$$a = \frac{R_L V_o}{(R_i + R_L)} \qquad [1b]$$

and

$$b = \frac{1}{(R_i + R_L)C} \qquad [1c]$$

where V_o is the charging voltage, R_i is the cell internal resistance, R_L is the load resistance and C is the cell capacitance. The semilogarithmic plot of V_L vs. t would be a straight line. Clearly this is not the case here. The curvature of the line in Figure 7b indicates a process with more than one time constant.

Figure 7a

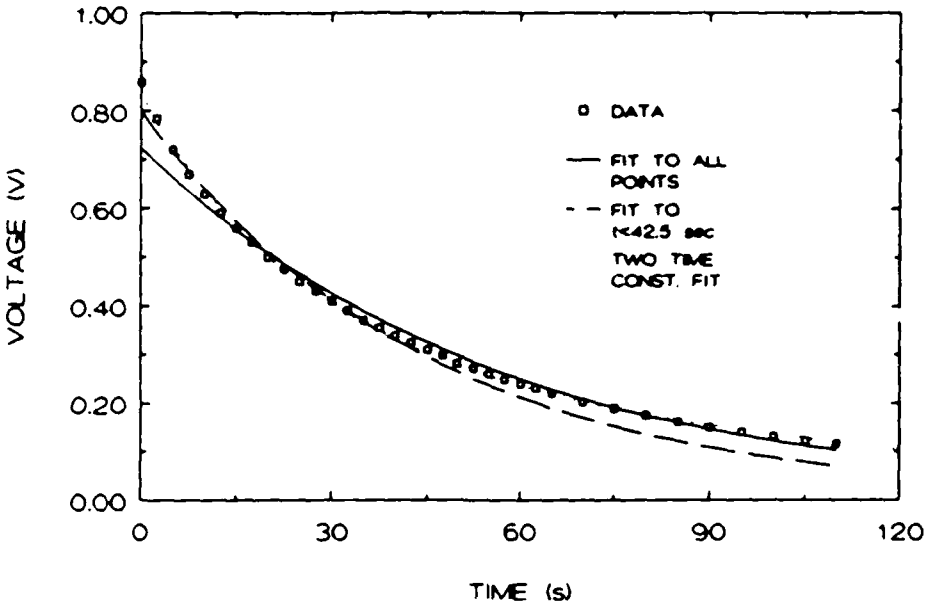

Figure 7b

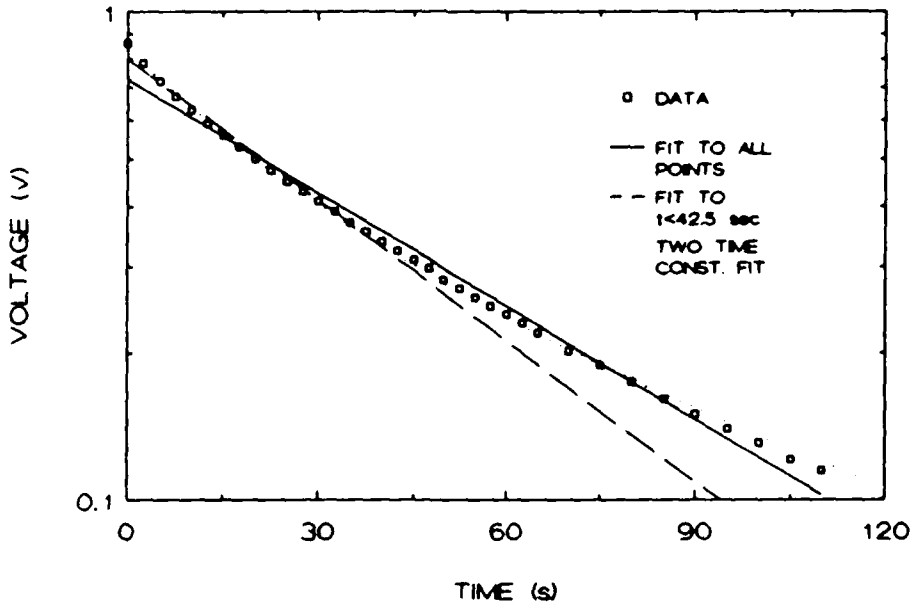

Figure 7: Discharge of M and E 369-38-1 across a 100-Ω Load, a) Voltage vs. t, b) Log V vs. t.

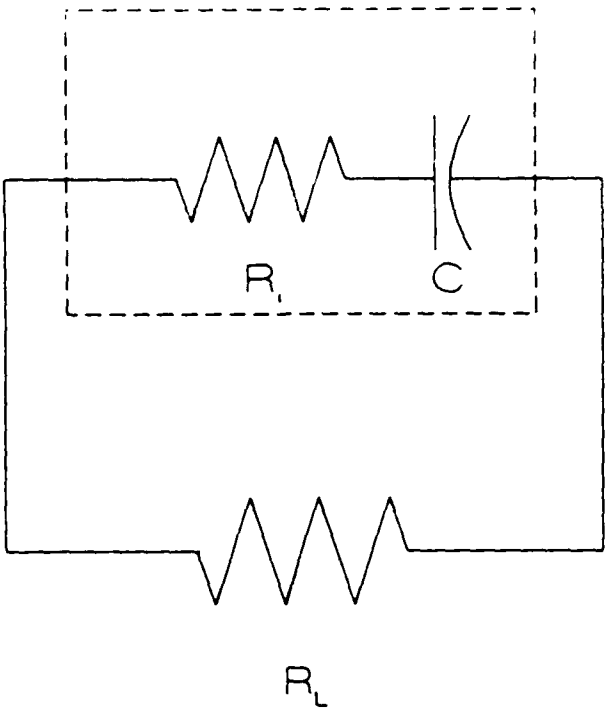

Figure 8: Equivalent Circuit of a Capacitor with Capacitance, C, and Internal Resistance, R_i, Discharging Across a Load Resistance, R_L.

Due to the non-ideal capacitive behavior of the system, different values of capacitance can be derived depending on the data analysis method. **Table III** lists the various values obtained by the different methods. The one-point method uses the time it takes for the voltage to decay from V_i to V_i/e as the time constant. The capacitance is then computed from the time constant:

$$C = \tau/R_t \qquad [2]$$

This yields a capacitance of 0.422 F.

Table III - Calculated Capacitances

Method	Capacitance
Decay to 1e	0.422 F
NLLS* to Full Data Set	0.560 F
NLLS to 42.5 sec	0.449 F
By Integration to 110 sec	0.391 F

* Non-Linear Least-Squares Fit

A non-linear least-squares fit in the form of Equation 1 to the full data set yields:

$$V_L = 0.726 \exp(-t/56.1) \quad [3]$$

and using Equation 2 a capacitance of 0.56 F is derived. However, Equation 3 does not fit the early time data very well.

A fit to the early time data (t <42.5 sec) yields:

$$V_L = 0.800 \exp(-t/45.2) \quad [4]$$

and using Equation 2 a capacitance of 0.449 F is derived. Equation 4 does not fit the longer time data very well. We see a trend of lower capacitance when data at shorter times are used. This is consistent with the very low capacitance value observed at higher frequencies using impedance methods, as discussed earlier.

An integral capacitance can be computed from:

$$C = q/V_o \quad [5]$$

the charge is obtained by integrating the current:

$$q = \int i dt = \int \frac{V_L}{R_L} dt \quad [6]$$

The charge delivered by the cell (to 110 sec) is 0.352 C (integrating Figure 7a by the trapezoidal rule). The integral capacity is 0.391 F. Since the cell was not fully discharged at 110 sec, this is less than the true integral capacity.

The data can also be fit to the more complex expression:

$$V_L = a*(e^{-bt} + e^{-dt}) \quad [7]$$

For the data of Figure 7, a = 0.4190, b = 1/22.3 and d = 1/86.2. This expression fits the data very well. The best value for the capacitance appears to be 0.42 F.

4. FUTURE WORK

The internal resistance will eventually limit the power delivery capability of the cell. We will be working on methods to lower the cell internal resistance.

We have begun to transition into testing cells of 2" x 2" size. This requires that methods be developed to make consistent M and Es (with respect to capacitance and internal resistance) of this size. During the next quarter, we will be evaluating several fabrication methods.

5. REFERENCES

Abbey, Kyzburz, Abstract #655, Extended Abstracts, Vol. 89-2, 176th ECS Meeting, Fall 1989, Hollywood, Florida

Balko, E.N., C.R. Davidson and A.B. LaConti, *J. Inorg. Nucl. Chem.*, **42**, 1778 (1980).

Rishpon, and S. Gotterfeld, *J. Electrochem. Soc.*, **131**, 1960 (1984).